Low Computational Complexity for Optimizing Energy Efficiency in mm-wave Hybrid Precoding System for 5G

ADEB SALH[1], LUKMAN AUDAH[1],
QAZWAN ABDULLAH[1,2,3], (Graduate Student Member, IEEE),
ÖMER AYDOĞDU[2], MOHAMMED A. ALHARTOMI[4], (Member, IEEE),
SAEED HAMOOD ALSAMHI[5,6], FARIS A. ALMALKI[7],
AND NOR SHAHIDA M. SHAH[1]

[1]Wireless and Radio Science Centre (WARAS), Faculty of Electrical and Electronic Engineering, Universiti Tun Hussein Onn Malaysia, Parit Raja, Batu Pahat, Johor 86400, Malaysia
[2]Faculty of Engineering and Natural Sciences, Konya Technical University, 42250 Konya, Turkey
[3]Faculty of Electrical and Electronic Engineering, Selçuk University, 42250 Konya, Turkey
[4]Department of Electrical Engineering, University of Tabuk, Tabuk 47512, Saudi Arabia
[5]SRI, Technological University of the Shannon: Midlands Midwest, Athlone, Westmeath, N37 F6D7 Ireland
[6]Faculty of Engineering, IBB University, Ibb, Yemen
[7]Department of Computer Engineering, College of Computers and Information Technology, Taif University, Taif 21944, Saudi Arabia

Corresponding authors: Lukman Audah (hanif@uthm.edu.my) and Qazwan Abdullah (gazwan20062015@gmail.com)

ABSTRACT Millimeter-wave (mm-wave) communication is the spectral frontier to meet the anticipated significant volume of high data traffic processing in next-generation systems. The primary challenges in mm-wave can be overcome by reducing complexity and power consumption by large antenna arrays for massive multiple-input multiple-output (mMIMO) systems. However, the circuit power consumption is expected to increase rapidly. The precoding in mm-wave mMIMO systems cannot be successfully achieved at baseband using digital precoders, owing to the high cost and power consumption of signal mixers and analog-to-digital converters. Nevertheless, hybrid analog–digital precoders are considered a cost-effective solution. In this work, we introduce a novel method for optimizing energy efficiency (EE) in the upper-bound multiuser (MU) - mMIMO system and the cost efficiency of quantized hybrid precoding (HP) design. We propose effective alternating minimization algorithms based on the zero gradient method to establish fully-connected structures (FCSs) and partially-connected structures (PCSs). In the alternating minimization algorithms, low complexity is proposed by enforcing an orthogonal constraint on the digital precoders to realize the joint optimization of computational complexity and communication power. Therefore, the alternating minimization algorithm enhances HP by improving the performance of the FCS through advanced phase extraction, which involves high complexity. Meanwhile, the alternating minimization algorithm develops a PCS to achieve low complexity using HP. The simulation results demonstrate that the proposed algorithm for MU - mMIMO systems improves EE. The power-saving ratio is also enhanced for PCS and FCS by 48.3% and 17.12%, respectively.

INDEX TERMS mm-wave, MIMO, energy efficiency, fully connected structure, partially connected structure.

I. INTRODUCTION

The massive multiple-input multiple-output (mMIMO) system operations on millimeter-wave (mm-wave) aims to meet

the anticipated emergence as key solutions and growth of traffic demands for high-data-rate multimedia access in fifth-generation (5G) systems [1]–[3].

The growing mobile data traffic, such as those from smartphone and mobile internet users, can be supported through

The associate editor coordinating the review of this manuscript and approving it for publication was Fan-Hsun Tseng.

A. Salh *et al.*: Low Computational Complexity for Optimizing Energy Efficiency in mm-wave Hybrid Precoding System for 5G

IEEE *Access*

the availability of more bandwidth, which offers higher data rates for all users and capacity in a mobile cellular network. Consequently, mm-wave has a frequency that ranges between 30 and 300 GHz, which provides gigabit-per-second data rates in 5G wireless systems. High propagation loss and rain attenuation are the main limitations that cause the attenuation at transmitting signals in mm-wave frequencies. The considerable beamforming gain can be decreased by reducing the propagation loss, and the highly directional beam can be generated by deploying the small wavelength of mm-wave signals. The energy cost and hardware complexity of digital precoders (DPs) increase when the number of antennas is large. Reducing the cost, power consumption (PC), and the number of radio frequency (RF) chains cannot realize precoding only by using DPs at baseband in [4] or only using analog precoding, which uses phase shifters in [5].

The hybrid precoding (HP) architecture for mm-wave mMIMO systems is a newly emerging technique that enables directional beamforming with large antenna arrays to improve energy efficiency (EE). It jointly enhances the computation and PC by means of two different HP architectures in RF systems equipped with fully connected structures (FCSs) and partially connected structures (PCSs). The minimum data rate of users in the former can be maximized by connecting every RF chain (FCS) by phase shifters to activate the large spatial degree of freedom gain [6]–[14]. HPs based on orthogonal matching pursuit (OMP) algorithm exhibit a reasonably good performance by studying the sparsity constrained matrix reconstruction problem [5], [6]. Hybrid precoders based on phase-shifting topologies with OMP algorithm are shown to provide a decent performance by investigating the sparsity reconstruction to increase EE full resolution of quantized HP provided with FCS phase shifting in [7]. The simulation results confirm that phase shifting enhances spectral efficiency (SE) and may plausibly result in EE regression with extra bits in digital–analog converters. Tradeoffs between computational complexity and performance are demonstrated in [8] by improving four different algorithms for single-user HP and combiner. An algorithm that iteratively updates hybrid transceiver design for phases in the RF precoders or combiner is proposed in [9]. This approach achieves a near-identical rate in mm-wave between the full-baseband and the HP. A two-loop iterative algorithm and two sparse RF chain structures are also developed in [10] to decrease energy consumption by inserting auxiliary variables and employing successive convex approximation. This two-loop iterative algorithm aims to develop a sparse RF chain antenna at the base station (BS) and HP design to increase the EE of FCS/PCS. The nearly optimal low-complexity FCS RF precoding and combining in wideband are investigated in [12]. The proposed algorithm aims to attain higher EE by decreasing the correlation among different users and developing the unitary matrix quality of subarrays. Low-complexity hybrid block diagonalization is proposed for the downlink (DL) in [11] by employing the RF precoding to harvest the high array gain through phase-only RF precoding.

In harvesting the large array gain through a phase for only RF precoding, the target capacity is achieved by performing low-cost hybrid block [11]. It is shown in [13] that when the number of data streams (N_s) is more than twice the number of RF chains (N_{RF}), the energy-efficient HP achieves the global maximum EE. The FCS presented in [14], [15] involves a heuristic algorithm to solve the precoding problem, RF chains, and baseband processing to trade off the energy and cost efficiency in the RF chain circuits.

However, PCSs can reduce the hardware complexity for practical implementation by connecting every RF chain that is only connected to a limited number of antennas [14]–[19]. Corresponding to the PCS, the antenna arrays at the BS consist of multiple subarrays, which entail a lower hardware complexity than the FCS [14]. The proposed matrix of factorizing based on a near-optimal design for every subarray is investigated under the effects of the number of subarrays and RF chains. The simulation results in [14] show that the proposed algorithm reduces SE for FCS/PCS with an increased N_{RF}. The N_{RF} does not need to be increased according to [15] as it will increase cost and PC. The authors in [15] proposed alternating minimization algorithms for FCS/PCS that optimize the DPs and the analog precoders. The simulation results reveal that the PCS can outperform the FCS in terms of a higher EE and lower-complexity hardware with a large N_{RF}. The transmission rate can be improved by addressing the tradeoff between performance and hardware efficiency by employing the FCS/PCS with dynamic subarray and low-resolution phase shifters. This approach proposes an iterative hybrid beamformer design to mitigate the performance loss by fixed subarrays connected for every RF chain to all transmission antennas [17]. The optimal HP in [18] proposes a PCS to bypass the hardware constraint on the analog phase. This PCS jointly designs the optimal unconstrained precoders by optimizing the analog and DPs to reduce the required RF chain. Implementing signal processing in the baseband and allocating an RF chain per antenna are difficult because of the resulting high cost and PC. The energy-efficient maximization based on solving the analog precoders and combiner problem is optimized in [19] through the alternating direction optimization method in a sub-connected structure. Decreasing the circuit complexity effect on circuit PC and efficiency has not been attempted yet. EE is maximized in [20] by finding low-complexity transmission by improving the Doherty power amplifier for FCS/PCS with low complexity. This development for power amplifiers depends on studying the beam-steering codebook and baseband zero-forcing digital beamformer to maximize the EE. Motivated by the abovementioned gap, we optimize EE and offer low computational complexity based on updating a phase extraction for constraint transmission power and zero gradient-based iterative minimization algorithms, which increase the N_s compared with more RF chains in FCS and a PCS. However, from the abovementioned gap, the performance of FCS and PCS cannot be achieved compared to the N_s because the semidefinite relaxation program, alternating

IEEE Access·

A. Salh *et al.*: Low Computational Complexity for Optimizing Energy Efficiency in mm-wave Hybrid Precoding System for 5G

TABLE 1. Summary of notations and abbreviations.

LIST OF NOTATIONS

$\mathfrak{F}^{RF}$	The analog RF precoding vector achieved phase shifters
$\mathfrak{F}^{BB}_k$	The BBP matrix for the k th UE
$\mathfrak{F}^{SS}_k$	Unitary precoding matrix
$\hbar_k$	The DL channel matrix
$\mathfrak{F}^{opt}$	The optimal BBP
$\acute{o}_k$	The complex white Gaussian noise
N_t	The number of transmit antennas array at the BS
N_r	The number of antennas array at UE
N_s	The transmitter data streams
$\Omega_{k,l}$	The complex channel gain of the k th UE
$\mathcal{L}_k$	The number of multi-paths propagation channel of the k th UE
Γ_i	The received interference and noise power of the kth UE
$\mathfrak{p}_t$	Power consumption
$\mathfrak{p}_{Communi}$	The communication power
$\mathfrak{p}_{PA}$	The power consumed by power amplifiers
$\mathfrak{P}_{RF}$	The power consumed at every RF chain
$\mathfrak{p}_C$	The circuit PC is affected by baseband signal processing
ϖ	The bandwidth transmission of the k th UE
$\mathfrak{r}_k$	The available data rate at k th data stream of UE
γ	The iterative step
$Q^{(i)}_k$	Hermitian symmetric positive
$\mathfrak{C}\mathfrak{I}$	A symmetric positive definite matrix

LIST OF ABBREVIATIONS

mMIMO	Massive multiple-input multiple-output
EE	Energy efficiency
HP	Hybrid precoding
PCS	Partially connected structures
FCS	Fully connected structures
BS	Base station
PC	Power consumption
BBP	baseband precoding
DPs	digital precoders
RF	Radio frequency
5G	Fifth-generation
QCQP	Quadratic constraint quadratic programming
DL	Downlink
SE	Spectral efficiency

direction optimization method, and OMP algorithms do not have lower complexity, thereby allowing the N_{RF} to increase and become inconvenient while estimating channels for a given RF [15]–[19].

The main objective of this study is to improve the EE by reducing the cost, PC, and number of RFs, based on the proposed effective alternating minimization algorithms to establish FCSs and PCSs. The FCS of HP design is performed by updating a phase extraction for constraint transmission power and zero gradient-based iterative minimization algorithms to reduce the hardware complexity of the fully DP as long as the N_{RF} is comparable to the N_s. On the other hand, the PCS–HP matrix is proposed to optimize EE and provide a low hardware complexity in mm-wave by employing fewer phase shifters in the analog RF precoders to optimize baseband precoding (BBP) and decrease the hardware complexity in the RF chains domain.

All the notations and abbreviation are listed in Table 1.

A. CONTRIBUTIONS
Comprehensive achievement evaluation of quantized HP design in mm-wave MIMO systems with FCS/PCS depends

on proposing alternating minimization algorithms for solving the problem of HP and optimizing the digital and analog precoders. The optimal solutions for designing a PCS for HPs are offered by decreasing the Euclidean distance between analog RF and BBPs. This approach decreases the hardware complexity in the RF chains domain with low-cost phase shifters. The optimal HP design is proposed with novel PCS based on adopting the notation quadratic constraint quadratic programming (QCQP) with low-complexity HP for alternating minimization algorithm to avoid high energy consumption. In addition, an optimal HP design is proposed with novel PCS, which provides high resolution and considerable gain for analog beamforming, generates a relatively large N_{RF}, and maximizes EE. The contributions of this study are summarized as follows:

- The optimal HP design problem for mm-wave mMIMO systems is investigated using the orthogonal property of the DPs for an FCS and a PCS by employing fewer phase shifters in the analog RF precoders to attain high EE.

- Energy- and cost-efficient optimization solutions are proposed by formulating the design of hybrid RF chains of energy consumption and BBP matrix to adopt upper-bound energy-efficient solutions for 5G mm-wave mMIMO systems.

- Low computational complexity and small performance loss are achieved by applying columns of the unconstrained property of the mutually orthogonal optimal precoding matrix by using the square of the Frobenius norm in the upper bound. An FCS of HP design is performed by updating a phase extraction for constraint transmission power, and zero gradient-based iterative minimization algorithms are improved by enforcing an orthogonal constraint on the DPs. Thus, the joint optimization of computational complexity and communication power is realized.

II. SYSTEM MODEL
A. MULTIUSER HP FOR WIRELESS TRANSMISSION MODEL
We consider the DL transmission for the mm-wave MU- mMIMO system of FCS/PCS based on HP, as shown in Fig. 1. We assume that the HP is the perfect channel state information (CSI) known at the transmitter and receiver [20]–[24]. The transmitter sends N_s data streams and collects transmission antennas N_t, and every user is equipped with N_r. Each active user (UE) has a single N_{RF} connected to an antenna element. Consequently, one data stream can be supported by each user. The transmitter is equipped with N_{RF} to support each antenna element data stream N_s from N_t transmission antennas to N_r receiver antennas simultaneously as $N_s \leq N_{RF} \ll N_t$. The received signal at $\mathcal{Y}_k \in \mathbb{C}^{N_r \times N_t}$ UE in the HP - mMIMO system can be expressed as:

$$\mathcal{Y}_k = \hbar_k^H \mathfrak{F}^{RF} \mathfrak{F}^{BB}_k u_k + \acute{o}_k \tag{1}$$

The vector transmitted signal u_k from the BS to user $u_k = [u_1, \ldots, u_k \ldots, u_K] \in \mathbb{C}^{N_s \times 1}$, and $\hbar_k \in \mathbb{C}^{N_r \times N_t}$ is the channel vector matrix $\hbar_k$ from BS to UE. $\mathfrak{F}^{BB}_k \in \mathbb{C}^{N_{RF} \times K}$ is

A. Salh *et al.*: Low Computational Complexity for Optimizing Energy Efficiency in mm-wave Hybrid Precoding System for 5G
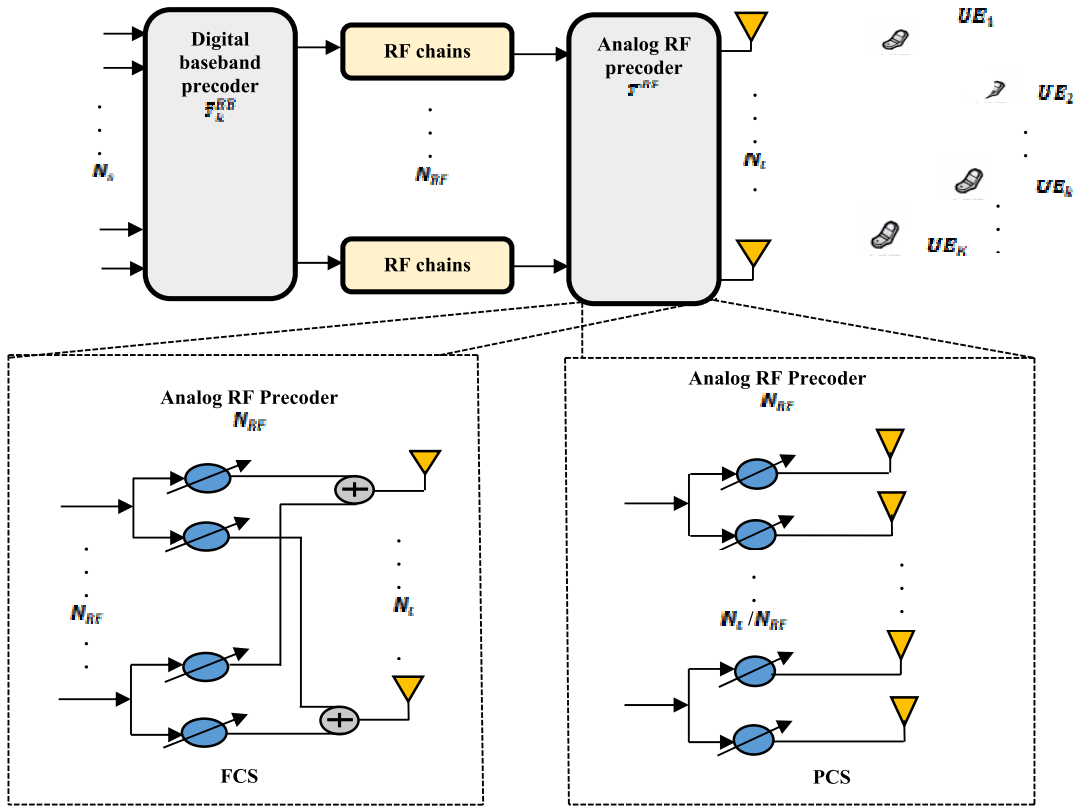
IEEE *Access*

FIGURE 1. Hybrid precoding in mm-wave MU - mMIMO systems.

the BBP matrix for the k th user, where the k th column of $\mathcal{F}_k^{BB}$ is expressed as $\mathfrak{f}_k^{BB}$. $\eth_k \mathbb{C} \mathcal{N} \left(0, \alpha^2\right)$ is the complex white Gaussian noise (AWGN) vector, and α_n^2 represents the noise power. $\mathcal{F}^{RF} \in \mathbb{C}^{N_t \times N_{RF}}$ is the analog RF precoding vector achieved by N_t phase shifters. Moreover, the analog RF and BBPs can fulfill the received power constraint $\left\| \mathcal{F}^{RF} \mathcal{F}_k^{BB} \right\|_F^2 \leq P$.

B. MILLIMETER-WAVE CHANNEL MODEL

The channel modeling of the mm-wave propagation channel is supported through the extreme high antenna correlation. The channel propagation loss is extreme compared with that in the low-band channel with the fully dispersed environment to adopt the CSI with L path propagation in transmitting a signal from BS to every user. The DL channel matrix can be expressed as follows:

$$\hbar_k = \sqrt{\frac{N_r N_t}{\mathcal{L}_k}} \sum_{l=1}^{\mathcal{L}_k} \Omega_{k,l} \grave{a} \left(\phi_{k,l}^r\right) \grave{a} \left(\phi_{k,l}^t\right)^T \quad \forall k \quad (2)$$

where N_t is the number of transmit antennas array at the BS, N_r is the number of antennas array at UE, $\Omega_{k,l}$ is the complex channel gain of the k th UE over the l th multi-path, which includes the path loss with $\mathbb{E}\left|\Omega_{k,l}\right|^2 = 1$, and $\mathcal{L}_k$ is the number of multi-paths propagation channel of the k th user $l \in [1, 2, ..\mathcal{L}_k]$. $\grave{a}_t \left(\phi_{k,l}^r\right)$ and $\grave{a}_t \left(\phi_{k,l}^t\right)$ represent the normalized transmit and receive array response vector for the azimuth angles of arrival $\phi_{k,l}^r$, and $\phi_{k,l}^t$ of the l th multi-path

propagation, respectively. The array response vector for the N- element of a uniform linear array can be written as:

$$\grave{a}_{ULA} \left(\phi_{k,l}^r\right) = \frac{1}{\sqrt{N}} \left[1, e^{j\frac{2\pi}{\gamma} \sin\phi}, \ldots, e^{-j\frac{2\pi d(N-1)}{\gamma} \sin\phi}\right]^T \quad (3)$$

where N represents the number of antenna elements equipped with the BS, γ is the wavelength of carrier frequency, and $d = \frac{2}{\gamma}$ represents the inter distance for antenna elements. Every mm-wave can save energy by controlling the beam direction at transmitting beam from N_{RF} BSs to serving the k th UE. The sidelobe beam creates an analog beamforming vector based on a signal-to-interference noise ratio. The available data rate at k th data stream of UE can be written as:

$$\mathcal{r}_k$$
$$= \varpi \sum_{k=1}^{K} \log_2 (1$$
$$+ \frac{\left| \hbar_k^H \mathfrak{f}_k^{BB} \left(\mathfrak{f}_k^{BB}\right)^H \mathcal{F}^{RF} \left(\mathcal{F}^{RF}\right)^H \hbar_k \right|^2}{\sum_{\substack{i \neq k \\ i=1}}^{K} \left| \sum_{k=1}^{K} \hbar_k^H \mathcal{F}^{RF} \mathfrak{f}_i^{BB} \left(\mathfrak{f}_i^{BB}\right)^H \left(\mathcal{F}^{RF}\right)^H \hbar_k \right|^2 + \alpha_n^2}) \quad (4)$$

where ϖ is the bandwidth transmission of the k th UE. We assume that every mm-wave BS achieves the low-dimensional processing with the BBPs to cancel inter-user

interference by defining $\hbar_k^H \mathcal{F}_k^{BB} = 0$ when $i \neq k$. The achievable data rate at k th UE can be written as

$$r_{sum} = \sum_{k=1}^{K} r_k \tag{5}$$

From (5), the BS transmitter has a perfect CSI to adopt with the precoding problem [21]–[24]. In practical scenarios, the channel reciprocities are the same through the uplink channel estimation and application of DL channels in the time division duplex [25]. The estimation of the mm-wave using pressed channel sensing is investigated in [26], [27].

III. PROBLEM FORMULATION
A. POWER MODEL
In mm-wave MU - mMIMO system, maximize the EE at the BS depend on optimizing BBP $\mathcal{F}_k^{BB}$ and RF precoding transmission systems $\mathcal{F}^{RF}$ need to be computed. In this case, the consumption power cannot be ignored. The PC at the transmitter consists of two parts: communication power and circuit PC. It can be written as follows:

$$P_t = P_{Communi} + P_C \tag{6}$$

The communication power in the first term in (6) consists of two parts $P_{Communi} = P_{PA} + P_{RF}$; P_{PA} is the power consumed by power amplifiers, and P_{RF} is the power consumed at every RF chain. The circuit PC P_C is affected by baseband signal processing, phase shifter [28], [19], cooling, and synchronization in the BS. The consumed power to transmit signal for the k th UEs by the power amplifier can be described mathematically as:

$$P_{PA} = \frac{1}{\Xi} \sum_{k=1}^{K} \left\| \mathcal{F}^{RF} \mathfrak{f}_k^{BB} \right\|_F^2 \tag{7}$$

where Ξ is the efficiency of the power amplifier, and $\sum_{k=1}^{K} \left\| \mathcal{F}^{RF} \mathcal{F}_k^{BB} \right\|_F^2$ is the power consumed to transmit signal for k th UE. We suppose equal power allocation between the baseband signals of different UEs. The power consumed P_{RF} by converters, mixers, filters, and phase shifters at every RF chain can be written as:

$$P_{RF} = N_{RF} P_{RF} \tag{8}$$

where P_{RF} is the PC by an RF chain. By substituting (7) and (8) into (6), the total PC can be expressed as follows:

$$P_t = \frac{1}{\Xi} \sum_{k=1}^{K} \left\| \mathcal{F}^{RF} \mathcal{F}_k^{BB} \right\|_F^2 + N_{RF} P_{RF} + P_C \tag{9}$$

B. ENERGY EFFICIENCY
Maximizing EE is of prime concern while designing the mm-wave MU - mMIMO system. The optimization problem for the maximization of EE can be defined mathematically as follows, (10), as shown at the bottom of the next page,

The EE in an MU - mMIMO system can be maximized by achieving a good tradeoff between the data rate and total PC

through jointly optimizing the BBP matrix $\mathcal{F}_{BB}$ and the RF precoding matrix $\mathcal{F}_{RF}$. This optimization is formed by

$$\max_{\mathcal{F}_{RF}, \mathcal{F}_{BB}} EE = \varpi \frac{\sum_{k=1}^{K} \overline{r_k}}{P_t}$$

$$\sum_{k=1}^{K} \left\| \mathcal{F}^{RF} \mathcal{F}_k^{BB} \right\|_F^2 \leq P_{max}$$
$$r_k \geq \Gamma_k, \quad k = 1, \dots, K$$
$$\left\| \mathcal{F}^{RF} \right\|_F^2 = \frac{1}{N_t} \tag{11}$$

where P_{max} is the total transmission power in the abovementioned constraints. Constraint (11) signifies that one BS should serve all UEs. $\sum_{k=1}^{K} \left\| \mathcal{F}^{RF} \mathcal{F}_k^{BB} \right\|_F^2 \leq P_{max}$ represents a non-convex constraint because of the analog precoding and digital precoding matrix connection.

The problem in (11), $\left\| \mathcal{F}^{RF} \right\|_F^2 = 1/N_t$, involves difficulty while solving for antenna selection because of the matrix variables $\mathcal{F}_{RF}$ and $\mathcal{F}_{BB}$. We propose that the HP matrix design approach achieves an optimum solution with less computational complexity to resolve this issue. As shown in [24], minimizing the objective function in (11) nearly advances to the maximization of the EE. Moreover, the optimal HPs must be closed to the unconstrained optimal BBP. Explicitly solving the baseband and RF precoding matrices is also difficult because of the complexity and non-concave properties of the optimization problem in (11). To solve this problem, we derive the upper bound on the EE.

C. UPPER BOUND OF EE
To derive the upper bound of EE, the EE optimization constraints are relaxed in (11) owing to the non-concavity of the EE, which is difficult to apply in (11) for finding the local maximum using Lagrange multipliers. Therefore, we use a zero gradient-based iterative algorithm to obtain an optimal BBP vector. Furthermore, simplifying the derivation is based on the BBP matrix and RF precoding matrix, where $\mathcal{F}_k^{BB} \in \mathbb{C}^{N_{RF} \times K}$ is related to the N_{RF} and $\mathcal{F}^{RF} \in \mathbb{C}^{N_t \times N_{RF}}$ is related to the fully digital precoding matrix: $\mathcal{F}^{opt} \in \mathbb{C}^{N_t \times K}$, $\mathcal{F}^{opt} = \mathcal{F}^{RF} \mathcal{F}_k^{BB}$ in the first term in (9), $\mathcal{F}^{opt} = [\mathfrak{f}_1, \mathfrak{f}_2, \dots \mathfrak{f}_k, \dots \mathfrak{f}_K]$, where the k th column of $\mathcal{F}^{opt}$ is expressed as $\mathfrak{f}_k$ representing the local optimization for BBP vector for the kth UE. The optimal solution of EE uses the zero gradient method to obtain the stationary point of an optimal BBP vector for EE $(\mathfrak{f}_1, \mathfrak{f}_2, \dots \mathfrak{f}_k)$ and $\overline{r_k}(\mathfrak{f}_1, \mathfrak{f}_2, \dots \mathfrak{f}_k)$ [29]–[31].

$$\mathcal{F}^{opt} = EE(\mathfrak{f}_1, \mathfrak{f}_2, \dots \mathfrak{f}_k)$$
$$= \arg \max_{\mathcal{F} \in \mathbb{C}^{N_t \times K}} EE = \frac{\varpi \overline{r_k}}{\Xi \sum_{k=1}^{K} \left\| \mathfrak{f}_j \right\|^2 + N_{RF} P_{RF} + P_C} \tag{12}$$

Considering the complexity and non-concave properties of the problem, the constraint of EE and optimization in (11) are relaxed. The EE is a non-concave function and difficult to apply using the traditional method for obtaining its

A. Salh *et al.*: Low Computational Complexity for Optimizing Energy Efficiency in mm-wave Hybrid Precoding System for 5G

IEEE *Access*

global solution, such as the Lagrange multiplier. EE can be maximized by optimizing the BBP matrix, where $\mathfrak{F}^{\text{opt}}$ constrained by the received interference and noise power of the *k*th user [31] is

$$\Gamma_i = \sum_{\substack{j\neq i \\ j=1}}^{K} \hbar_i^H \mathfrak{f}_j \left(\mathfrak{f}_j\right)^H \hbar_i + \alpha_n^2 \tag{13}$$

Based on (12), the data rate in the numerator and the transmission PC in the denominator are shown in (14) and (15), respectively.

$$\overline{r}_k = \log_2 \left(1 + \frac{\left| \sum_{k=1}^{K} \hbar_k^H \mathfrak{f}_k^{BB} \left(\mathfrak{f}_k^{BB}\right)^H \hbar_k \right|^2}{\sum_{\substack{i\neq k \\ i=1}}^{K} \left| \sum_{k=1}^{K} \hbar_k^H \mathfrak{f}_i^{BB} \left(\mathfrak{f}_i^{BB}\right)^H \hbar_k \right|^2 + \alpha_n^2} \right) \tag{14}$$

$$(\overline{\mathcal{P}}) = \Xi \sum_{k=1}^{K} \|\mathfrak{f}_k\|_F^2 + N_{RF} p_{RF} + p_C \tag{15}$$

From the first partial derivation of $\text{EE}(\mathfrak{f}_k) = \left(\sum_{k=1}^{K} \overline{r}_k / \mathcal{P}\right)$ in (12), the baseband beamforming $\mathfrak{F}^{\text{opt}} = [\mathfrak{f}_1, \mathfrak{f}_2, \ldots \mathfrak{f}_k, \ldots \mathfrak{f}_K]$. The gradient of $\text{EE}(\mathfrak{f}_k)$ and data rate $\overline{r}_k(\mathfrak{f}_k)$ of the baseband beamforming $\mathfrak{f}_k$ are derived by

$$\frac{\partial \text{EE}(\mathfrak{f}_k)}{\partial(\mathfrak{f}_k)} = \frac{2}{\overline{\mathcal{P}^2}} \left[\mathcal{Q}_k - \mathcal{T}_k\right] \mathfrak{f}_k \tag{16}$$

with

$$\mathcal{Q}_k = \overline{\mathcal{P}} \frac{\hbar_k \hbar_k^H}{\sum_{j=1}^{K} \hbar_k^H \mathfrak{f}_j \left(\mathfrak{f}_j\right)^H \hbar_k + \alpha_n^2} \tag{17}$$

$$\mathcal{T}_k = \frac{2}{\Xi} I_{N_{RF}} \left(\sum_{i=1}^{K} \overline{r}_i\right)$$
$$+ \frac{2}{\ln 2} \varpi \overline{\mathcal{P}} \sum_{\substack{i\neq k \\ i=1}}^{K} \frac{\hbar_i^H \mathfrak{f}_i (\mathfrak{f}_i)^H \hbar_i}{(\Gamma_i)^2 + \Gamma_i \hbar_i^H \mathfrak{f}_i (\mathfrak{f}_i)^H \hbar_i} . \hbar_i \hbar_i^H \tag{18}$$

The regulated beamforming vectors and the transmitted powers for all users can be improved by developing a zero gradient-based energy-efficient strategy. From an unconstraint optimization problem, the zero gradient condition $\mathfrak{f}_k$ must be satisfied when the partial derivation of $\frac{\partial \text{EE}(\mathfrak{f}_k)}{\partial(\mathfrak{f}_k)} = 0$. In this case, if $\mathfrak{f}_k$ is a stationary point, then the local optimization for the user can be expressed as:

$$\frac{\partial \text{EE}(\mathfrak{f}_k)}{\partial(\mathfrak{f}_k)} = \frac{2\left(\left[\mathcal{Q}_k - \mathcal{T}_k\right]\mathfrak{f}_k\right)}{\overline{\mathcal{P}^2}} = 0; \quad 1 \leq k \leq K \tag{19}$$

The global optimal solution is difficult to obtain, as illustrated in (11), where the EE is not convex/concave in the weighting vector. A zero gradient-based iterative algorithm is developed to obtain the optimal local solution. Therefore, the partial derivation of $\text{EE}(\mathfrak{f}_k)$ is achieved using the iterative algorithm as follows:

Algorithm 1 Energy Efficiency on Upper Bound of HP Design

---

1. Assuming $\mathfrak{F}^{(0)}$ as an arbitrary initial value of the digital precoding matrix, $\mathcal{Q}_k^{(0)}$ and $\mathcal{T}_k^{(0)}$ are computed by (16).
2. A superscript (*i*) is considered the *i*th iteration for all user $k = 1, \ldots, K$.
3. **Repeat**
4. Calculate $\mathcal{T}_k^{(i)}, \mathcal{Q}_k^{(i)}, k = 1, \ldots, K$ based on (13), (17), and (18).
5. Given that $\mathcal{Q}_k^{(i)}$ is a Hermitian symmetric positive. matrix, $\mathcal{Q}_k^{(i)}$ can be denoted by $\mathcal{Q}_k^{(i)} = \mho \mho^H$, where $\mho$ represents a symmetric positive definite matrix, if $\mathcal{C} = \mathcal{Q}_k^{(i)} \left[\mathcal{T}_k^{(i)}\right]^{-1} \mathfrak{f}_k^{(i)}$,
6. Compute $\left(\frac{\partial \text{EE}(\mathfrak{f}_k)}{\partial(\mathfrak{f}_k)}\right)^H \left(\mathcal{C} - \mathfrak{f}_k^{(i)}\right) = \left|\text{EE}(\mathfrak{f}_k^{(i)})\mathfrak{F}^{(i)}\right|^H \left(\mathcal{C} - \mathfrak{f}_k^{(i)}\right) = \frac{2}{\overline{\mathcal{P}}}\left|\mathfrak{f}_k^{(i)}\right|^H \left(\mho^{-1}\mathcal{Q}_k^{(i)} - \mathcal{Q}_k^{(i)}\right)^H \left(\mho^{-1}\mathcal{Q}_k^{(i)} - \mathcal{Q}_k^{(i)}\right)\mathfrak{f}_k^{(i)}$
7. **For** $\gamma = 0 : \mathbb{C} : 1$
8. **For** $k = 1 : K$
9. **Temp_** $\mathfrak{f}_k^{(i+1)(\gamma)} = \gamma \left[\mathcal{T}_k^{(i)}\right]^{-1} \left[\mathcal{Q}_k^{(i)}\mathfrak{f}_k^{(i)(\gamma)}\right] + (1-\gamma)\mathfrak{f}_k^{(i)(\gamma)}$
10. **End for** k
11. **End for** γ
12. Set **temp_** $\mathfrak{f}_k^{(i+1)(\gamma)}$ as the *k*th column to form the matrix **temp_** $\mathfrak{F}^{(i+1)(\gamma)}$
13. Compute the maximum EE $\left(\textbf{temp\_}\mathfrak{F}^{(i+1)(\gamma)}\right)$ and let $\mathfrak{F}^{(i+1)} = \textbf{temp\_}\mathfrak{F}^{(i+1)(\gamma)}$,
14. $i = i + 1$
15. **Until**
16. $\left\|\mathfrak{F}^{(i+1)} - \mathfrak{F}^{(i)}\right\|_F \leq \varepsilon$, // a stopping criterion is triggered
17. $\mathfrak{F}^{\text{opt}} = \mathfrak{F}^{(i+1)}$

---

where γ is the iterative step, $\mathbb{C}$ is the step length interval, and ε is the stopping trigger. Step (6) is Hermitian symmetric

$$EE = \frac{\varpi \sum_{k=1}^{K} \log_2\left(1 + \frac{\left|\sum_{k=1}^{K} \hbar_k^H \mathfrak{f}_k^{BB}\left(\mathfrak{f}_k^{BB}\right)^H \mathfrak{F}^{RF}\left(\mathfrak{F}^{RF}\right)^H \hbar_k\right|^2}{\sum_{\substack{i\neq k \\ i=1}}^{K}\left|\sum_{k=1}^{K} \hbar_k^H \mathfrak{F}^{RF}\mathfrak{f}_i^{BB}\left(\mathfrak{f}_i^{BB}\right)^H\left(\mathfrak{F}^{RF}\right)^H \hbar_k\right|^2 + \alpha_n^2}\right)}{\frac{1}{\Xi}\sum_{k=1}^{K}\left\|\mathfrak{F}^{RF}\mathfrak{F}_k^{BB}\right\|_F^2 + N_{RF}p_{RF} + p_C}; \quad k = 1, 2, \ldots K \tag{10}$$

IEEE *Access*

A. Salh *et al.*: Low Computational Complexity for Optimizing Energy Efficiency in mm-wave Hybrid Precoding System for 5G

positive low-complexity HP and $\left| EE(\mathfrak{f}_k^{(i)})\mathfrak{F}^{(i)} \right|^H \left(\mathcal{C} - \mathfrak{f}_k^{(i)} \right)$ for all $\mathfrak{f}_k^{(i)}$. The algorithm is formulated and satisfies all the values when the $\left| EE(\mathfrak{f}_k^{(i)})\mathfrak{F}^{(i)} \right|^H \left(\mathcal{C} - \mathfrak{f}_k^{(i)} \right) \geq 0$, while the left term in step (6) $\frac{2}{\mathcal{P}} \left| \mathfrak{f}_k^{(i)} \right|^H \left(\mathcal{C}\mathcal{D}^{-1}\mathcal{Q}_k^{(i)} - \mathcal{Q}_k^{(i)} \right)^H \left(\mathcal{C}\mathcal{D}^{-1}\mathcal{Q}_k^{(i)} - \mathcal{Q}_k^{(i)} \right) \mathfrak{f}_k^{(i)}$ is extremum point by starting from any $\mathfrak{f}_k^{(i)}$ and going in the direction of $\mathcal{C} - \mathfrak{f}_k^{(i)}$. The $EE(\mathfrak{f}_k^{(i)})\mathfrak{F}^{(i)}$ becomes a non-decreasing function for all $\mathfrak{f}_k^{(i)}$ and shifts to $\mathcal{C}$. If the fully digital precoding matrix $\mathfrak{f}_k$ is assumed to be a stationary point according to [32], then the upper bound of $EE(\mathfrak{F}^{(i)})$ can be determined. Moreover, the upper bound of $EE(\mathfrak{F}^{(i)})$ is convergent for MU - mMIMO, and the upper bound of EE is reached. We present the HP problem and solve the same using the FCS/PCS as follows.

D. PHASE EXTRACTION ALTERNATING MINIMIZATION FOR THE FCS

Developing a HP matrix design can achieve low computational complexity and small performance loss. The interference between the multi-path streams can be mitigated by applying columns of the unconstrained property of the mutually orthogonal optimal precoding matrix $\mathfrak{F}^{\text{opt}}$. To help greatly simplify the design of the analog precoders, this orthogonal restriction depends on the ability of the analog precoders $\mathfrak{F}^{RF}$ to get rid of the product form with the $\mathfrak{f}_k^{BB}$. The digital precoding matrix should be mutually orthogonal by using a unitary matrix $\sigma\mathfrak{F}_{k(:,j)}^{SS}$ with the same dimension as $\mathfrak{f}_k^{BB}$ as $\left(\mathfrak{f}_k^{BB} \right)_{(j,:)}^H \mathfrak{f}_{k(:,i)}^{BB} = \sigma\left(\mathfrak{F}_k^{SS} \right)_{(:,i)}^H \sigma\mathfrak{F}_{k(:,j)}^{SS}$, as shown in (11) and (20). The mutual orthogonal property of a digital precoding matrix $\mathfrak{f}_k^{BB}$ in HP is replaced with $\sigma\mathfrak{F}_k^{SS}$ in (11).

$$\left(\mathfrak{F}_k^{SS} \right)_{(:,i)}^H \mathfrak{F}_{k(:,j)}^{SS}$$
$$= \begin{cases} \sigma^2 I_{N_s}, & \text{user } k \text{ is servied by } BSj, \ i = j \\ 0, & otherwise i = 1, 2, ..I, \ j = 0, \ 1, ..J, \ i \neq j \\ & i, j = 1, 2 .... N_s \end{cases}$$

(20)

The objective function in (11) and (20) is optimized by minimizing the Euclidean distance between $\mathfrak{F}^{RF}\mathfrak{F}_k^{BB}$ and $\mathfrak{F}^{\text{opt}}$.

$$\left\| \mathfrak{F}^{opt} - \mathfrak{F}^{RF}\mathfrak{F}_k^{BB} \right\|_F^2$$
$$= Tr \left(\mathfrak{F}^{opt} \left(\mathfrak{F}^{opt} \right)^H \right) - Tr \left(\left(\mathfrak{F}^{opt} \right)^H \mathfrak{F}^{RF} \mathfrak{F}_k^{BB} \right)$$
$$- Tr \left(\left(\mathfrak{F}^{RF} \right)^H \mathfrak{F}^{op} \left(\mathfrak{F}_k^{BB} \right)^H \right)$$
$$+ Tr \left(\left(\mathfrak{F}^{RF} \right)^H \mathfrak{F}^{RF} \left(\mathfrak{F}_k^{BB} \right)^H \mathfrak{F}_k^{BB} \right)$$

$$\left\| \mathfrak{F}^{opt} - \mathfrak{F}^{RF}\mathfrak{F}_k^{BB} \right\|_F^2$$
$$= \left\| \mathfrak{F}^{op} \right\|_F^2 - 2\sigma\mathbb{R}Tr \left(\mathfrak{F}_k^{SS} \left(\mathfrak{F}^{opt} \right)^H \mathfrak{F}^{RF} \right) + \sigma^2 \left\| \mathfrak{F}^{RF}\mathfrak{F}_k^{SS} \right\|_F^2$$

(21)

The partial derivatives in (21) can be computed as:

$$\frac{\partial \left\| \mathfrak{F}^{opt} - \mathfrak{F}^{RF}\mathfrak{F}_k^{BB} \right\|_F^2}{\partial\sigma}$$
$$= 2\sigma \left\| \mathfrak{F}^{RF}\mathfrak{F}_k^{SS} \right\|_F^2 - 2\mathbb{R} \ Tr \left(\mathfrak{F}_k^{SS} \left(\mathfrak{F}^{opt} \right)^H \mathfrak{F}^{RF} \right)$$

$$\sigma = \frac{\mathbb{R} \ Tr \left(\mathfrak{F}_k^{SS} \left(\mathfrak{F}^{opt} \right)^H \mathfrak{F}^{RF} \right)}{\left\| \mathfrak{F}^{RF}\mathfrak{F}_k^{SS} \right\|_F^2}$$

(22)

The smallest value obtained in (21) when the objective function $\sigma = \frac{\mathbb{R} \ Tr \left(\mathfrak{F}_k^{SS} \left(\mathfrak{F}^{opt} \right)^H \mathfrak{F}^{RF} \right)}{\left\| \mathfrak{F}^{RF}\mathfrak{F}_k^{SS} \right\|_F^2}$ and the optimal fully DPs is $\left\| \mathfrak{F}^{op} \right\|_F^2 - \frac{\left\{ \mathbb{R} \ Tr \left(\mathfrak{F}_k^{SS} \left(\mathfrak{F}^{opt} \right)^H \mathfrak{F}^{RF} \right) \right\}^2}{\left\| \mathfrak{F}^{RF}\mathfrak{F}_k^{SS} \right\|_F^2}$. The small performance loss and reduction in computational complexity are obtained using the square of the Frobenius norm in the denominator $\left\| \mathfrak{F}^{RF}\mathfrak{F}_k^{SS} \right\|_F^2$ of the upper bound as:

$$\left\| \mathfrak{F}^{RF}\mathfrak{F}_k^{SS} \right\|_F^2 = \left(\mathfrak{F}_k^{SS} \left(\mathfrak{F}_k^{SS} \right)^H \left(\mathfrak{F}^{RF} \right)^H \mathfrak{F}^{RF} \right)$$
$$= Tr \left(\begin{array}{cc} I_{N_s} & \\ & 0 \end{array} \right) \mathcal{M}^H \left(\mathfrak{F}^{RF} \right)^H \mathfrak{F}^{RF} \mathcal{M}$$
$$\leq Tr \left\{ \mathcal{M}^H \left(\mathfrak{F}^{RF} \right)^H \mathfrak{F}^{RF} \mathcal{M} \right\} = \left\| \mathfrak{F}^{RF} \right\|_F^2$$

(23)

where $\mathfrak{F}_k^{SS} \left(\mathfrak{F}_k^{SS} \right)^H = Tr \left(\begin{array}{cc} I_{N_s} & \\ & 0 \end{array} \right) \mathcal{M}^H \mathcal{M}$ represents the singular value decomposition (SVD) of $\mathfrak{F}_k^{SS} \left(\mathfrak{F}_k^{SS} \right)^H$ and the different powers when $\mathfrak{F}^{RF} = N_s\mathfrak{F}_k^{SS}$ represents the square matrix. The RF precoding transmission system $\mathfrak{F}^{RF}$ finds a free product with the BBP matrix $\mathfrak{F}_k^{BB}$ based on selecting the constant term $\left(\frac{1}{2 \left\| \mathfrak{F}^{op} \right\|_F^2} - 1 \right) + \left\| \mathfrak{F}^{op} \right\|_F^2 + \frac{1}{2}$ to the compelled term and multiplying it by the positive constant term $2 \left\| \mathfrak{F}^{op} \right\|_F^2$. The objective function $\left\| \mathfrak{F}^{opt} - \mathfrak{F}^{RF}\mathfrak{F}_k^{BB} \right\|_F^2$ in (21) maximizes EE at the BS without enhancing the loss by adding the Frobenius norm in the upper bound $\left\| \mathfrak{F}^{RF}\mathfrak{F}_k^{SS} \right\|_F^2 = \left\| \mathfrak{F}^{RF} \right\|_F^2$ and reducing the complexity.

$$\left\| \mathfrak{F}^{op} \right\|_F^2 - 2\mathbb{R} \ Tr \left(\mathfrak{F}_k^{SS} \left(\mathfrak{F}^{opt} \right)^H \mathfrak{F}^{RF} \right) + \left\| \mathfrak{F}^{RF} \right\|_F^2$$
$$= Tr \left(\left(\mathfrak{F}^{RF} \right)^H \mathfrak{F}^{RF} \right) - 2\mathbb{R} \ Tr \left(\mathfrak{F}_k^{SS} \left(\mathfrak{F}^{opt} \right)^H \mathfrak{F}^{RF} \right)$$

A. Salh *et al.*: Low Computational Complexity for Optimizing Energy Efficiency in mm-wave Hybrid Precoding System for 5G

IEEE *Access*

$$+\text{Tr}\left(\mathcal{F}_k^{SS}\left(\mathcal{F}_k^{SS}\right)^H\left(\mathcal{F}^{opt}\right)^H\mathcal{F}^{opt}\right)$$

$$=\left\|\mathcal{F}^{opt}\left(\mathcal{F}_k^{SS}\right)^H-\mathcal{F}^{RF}\right\|_F^2 \tag{24}$$

As shown in (21), the computational complexity is still high. The upper bound adopted in (24) satisfies the constraint transmission power by updating a phase extraction-based alternating minimization algorithm. The updating in (24) as the objective function for the HP $\left\|\mathcal{F}^{opt}-\mathcal{F}^{RF}\mathcal{F}_k^{BB}\right\|_F^2$ is given as:

$$\min_{\mathcal{F}_{RF}\in\mathbb{C}^{N_t\times\mathcal{F}_{RF}},\ \mathcal{F}_k^{SS}\in\mathbb{C}^{N_{RF}\times N_s}}\left\|\mathcal{F}^{opt}\mathcal{F}_k^{SS}-\mathcal{F}^{RF}\right\|_F^2$$

$$s.t.\begin{cases}\left(\mathcal{F}_k^{SS}\right)^H_{(,:\ i)}\mathcal{F}_{k(:,\ j)}^{SS}=I_{N_s}\\\mathcal{F}^{RF}_{(,:\ i)(,:\ j)}=1\qquad\forall_{i,j}\end{cases} \tag{25}$$

According to (25), a unitary precoding matrix $\mathcal{F}_k^{SS}$ can be obtained by applying the precoding matrix $\mathcal{F}_k^{BB}$ with orthogonal columns. The analog precoding $\mathcal{F}^{RF}$ in (25) obtains free product form with mutual orthogonal digital precoding matrix $\mathcal{F}_k^{BB}$, which can assist and simplify the analog precoder design by using phase extraction alternating minimization algorithm. The closed-form solution can be expressed as follows:

$$\arg\mathcal{F}^{RF}=\arg\left(\mathcal{F}^{opt}\left(\mathcal{F}_k^{SS}\right)^H_{(,:\ i)}\right) \tag{26}$$

where $\arg\mathcal{F}^{RF}$ represents the phase of $\mathcal{F}^{RF}$ obtained from the phases of a corresponding precoder $\mathcal{F}^{opt}\mathcal{F}_k^{SS}$ if $\mathcal{F}^{RF}$ is fixed for the DPs. Therefore, the analog $\mathcal{F}^{RF}$ phases can be derived from the phases of an analogous $\mathcal{F}^{opt}\mathcal{F}_k^{SS}$ precoder. When $\mathcal{F}^{RF}$ is fixed, the optimization solution for DPs can be solved as

$$\min_{\mathcal{F}_k^{SS}\in\mathbb{C}^{N_{RF}\times N_s}}\left\|\mathcal{F}^{opt}\mathcal{F}_k^{SS}-\mathcal{F}^{RF}\right\|_F^2$$

$$s.t.\left(\mathcal{F}_k^{SS}\right)^H_{(,:\ i)}\mathcal{F}_{k(:,\ j)}^{SS}=I_{N_s} \tag{27}$$

On the basis of (27), only one optimization variable $\mathcal{F}_k^{SS}$ is obtained, and it is equal to:

$$\max_{\mathcal{F}_k^{SS}\in\mathbb{C}^{N_{RF}\times N_s}}\mathbb{R}\ \text{Tr}\left(\mathcal{F}_k^{SS}\left(\mathcal{F}^{opt}\right)^H\mathcal{F}^{RF}\right)$$

$$s.t.\left(\mathcal{F}_k^{SS}\right)^H_{(,:\ i)}\mathcal{F}_{k(:,\ j)}^{SS}=I_{N_s} \tag{28}$$

In accordance with (28), we use the dual norm for the phases of an equivalent precoder $\mathcal{F}^{opt}\mathcal{F}_k^{SS}$ and phases of $\mathcal{F}^{RF}$ as:

$$\mathbb{R}\ \text{Tr}\left(\mathcal{F}_k^{SS}\left(\mathcal{F}^{opt}\right)^H\mathcal{F}^{RF}\right)$$

$$\leq\left|\text{Tr}\left(\mathcal{F}_k^{SS}\left(\mathcal{F}^{opt}\right)^H\mathcal{F}^{RF}\right)\right|$$

$$\leq\left\|\left(\mathcal{F}_k^{SS}\right)^H\right\|_\infty\cdot\left\|\left(\left(\mathcal{F}^{opt}\right)^H\mathcal{F}^{RF}\right)\right\|_1$$

$$=\left\|\left(\left(\mathcal{F}^{opt}\right)^H\mathcal{F}^{RF}\right)\right\|_1=\sum_{i=1}^{N_s}\alpha_i \tag{29}$$

where $\|.\|_\infty$ represents the stand infinite norm and $\|.\|_1$ represents one Schatten norm. The equality is determined only according to (29) when $\mathcal{F}_k^{SS}=\mathbb{v}_1\mathbb{y}^H$, where $\left(\left(\mathcal{F}^{opt}\right)^H\mathcal{F}^{RF}\right)=\mathbb{v}\sum\mathbb{y}^H$ is FCS in HP. Moreover, the optimal HP $\left(\mathcal{F}^{opt}\right)^H\mathcal{F}^{RF}=\mathbb{v}\ \mathbb{s}\ \mathbb{y}_1^H$, which is the SVD of $\left(\mathcal{F}^{opt}\right)^H\mathcal{F}^{RF}$, and $\mathbb{s}$ represents diagonal matrix with elements that are the first N_s non-zero singular values according to (33) $\alpha_1,\dots\dots\alpha_{N_s}$. As per (29), the value of α is determined according to the construct a matrix $\mathcal{F}_k^{BB}$ related to every $\mathcal{F}_k^{SS}$, where the exact normalization $\mathcal{F}_k^{SS}$ fulfills the power constraint by reducing the complexity of the phase extraction for alternating minimization algorithm.

Algorithm 2 Optimized HP-Based Phase Extraction Alternating Minimization for the FCS

---

1. **Input**: $\mathcal{F}^{opt}$
2. Establish $\mathcal{F}_0^{RF}$ and set $i=0$;
3. **Repeat**
4. Fix $\mathcal{F}_i^{RF}$, and calculate the SVD of $\left(\mathcal{F}^{opt}\right)^H\mathcal{F}^{RF}_{(,:\ i)}=\mathbb{v}^i\mathbb{s}^i\mathbb{y}_1^{i\ H}$;
5. Establish $\mathcal{F}_{k(i,\ :)}^{SS}=\mathbb{v}_1^i\mathbb{y}_i^H$;
6. Fix $\mathcal{F}_{k(i,\ :)}^{SS}$, and optimize the HP matrices according to (27) $\arg\mathcal{F}_{i+1}^{RF}=\arg\left(\mathcal{F}^{opt}\left(\mathcal{F}_k^{SS}\right)^H_{(,:\ i)}\right)$;
7. $i=i+1$;
8. **Until** stopping criterion is triggered;
9. For a DP at the end of the transmission, $\mathcal{F}_k^{BB}=\mathcal{F}_k^{SS}\sqrt{N_s}/\left\|\mathcal{F}^{RF}\mathcal{F}_k^{SS}\right\|_F$.

E. LOW-COMPLEXITY HP ALTERNATING MINIMIZATION FOR THE PCS

This section proposes the PCS–HP matrix design to optimize EE and provide low hardware complexity in mm-wave by employing fewer phase shifters in the analog RF precoders. The EE in MU - mMIMO system will conduct optimization when the creation of HP matrices $\mathcal{F}^{RF}\mathcal{F}_k^{BB}$ approaches the upper bound with the partially digital precoding matrix $\mathcal{F}^{opt}$. In PCS, every RF is connected to a convincing number of antennas by employing a minimization Euclidean distance between $\mathcal{F}^{RF}\mathcal{F}_k^{BB}$ and $\mathcal{F}^{opt}$, which are used to solve and optimize baseband and RF precoding matrices $\mathcal{F}^{RF}_{opt}$ and $\mathcal{F}^{BB}_{opt}$ according to [8], [20], [22].

$$\max_{\mathcal{F}_{RF}\in\mathbb{C}^{N_t\times\mathcal{F}_{RF}},\ \mathcal{F}_{BB\in\mathbb{C}^{N_{RF}\times K}}}\left\|\mathcal{F}^{opt}-\mathcal{F}^{RF}\mathcal{F}_k^{BB}\right\|_F^2$$

$$s.t.\quad\mathcal{F}^{RF}=\text{diag}\left\{\mathfrak{f}_1,..,\mathfrak{f}_{N_{RF}}\right\}$$

$$\left\|\mathcal{F}^{RF}\mathcal{F}_k^{BB}\right\|_F^2\leq\text{P}_{max} \tag{30}$$

where $\mathfrak{F}^{opt}$ is the optimal BBP for the kth user. The hardware complexity in the RF chains domain can be decreased using every RF chain only connected with N_t/N_{RF}. According to (30), every RF chain is supplied with an antenna subarray to guarantee the total PC and multiplexing gain determined by the active RF chains and the dimension of PCS $\mathfrak{F}^{RF}$ as:

$$\mathfrak{F}^{RF} = \begin{bmatrix} \mathfrak{f}_1^{RF} & 0 & 0 \\ 0 & \ddots & 0 \\ 0 & 0 & \mathfrak{f}_{N_{RF}}^{RF} \end{bmatrix} \quad (31)$$

where $\mathfrak{f}_i = [i = 1, 2, \ldots,] \in \mathbb{C}^{N_{arry} \times 1}$ represents the analog precoding vector $\mathfrak{F}^{RF}$ to the i th subarray. The block diagonal $\mathfrak{f}_i$ represents the i th block matrix, which matches the precoding matrix between the ith RF chain and PCS N_t/N_{RF} antennas. Optimizing the BBP matrix $\mathfrak{F}_k^{BB}$ and minimizing the number of RF chain precoding matrix N_{RF} can maximize EE at the BS without any loss. In this section, we propose the alternating minimization method for communication power to optimize baseband because of the different structures of the constraint on $\mathfrak{F}^{RF}$ in the product $\mathfrak{F}^{RF}\mathfrak{F}_k^{BB}$ by fixing the $\mathfrak{F}^{RF}$ and obtaining a good solution for $\mathfrak{F}_k^{BB}$ as [33], [34].

$$\min_{\mathfrak{F}_{BB}\in\mathbb{C}^{N_{RF}\times K}} \left\| \mathfrak{F}^{opt} - \mathfrak{F}^{RF}\mathfrak{F}_k^{BB} \right\|_F^2$$

$$s.t. \left\| \mathfrak{F}^{RF}\mathfrak{F}_k^{BB} \right\|_F^2 \leq \mathsf{P}_{max} \quad (32)$$

We presume that (32) is a non-convex constraint according to channel in BS antenna arrays in (2) and from [15], [35] QCQP problem. Let $Ð = vec\left(\mathfrak{F}_k^{BB}\right)$ and $\mathfrak{f}^{opt} = vec\left(\mathfrak{F}^{opt}\right)$ and $\mathfrak{I} = I_{N_s}\otimes\mathfrak{F}^{RF}$. From the vectorization property, the objective function $\left\| \mathfrak{F}^{opt} - \mathfrak{F}^{RF}\mathfrak{F}_k^{BB} \right\|_F^2 = \left\| vec\left(\mathfrak{F}^{opt}\right) - \mathfrak{F}^{RF}\mathfrak{F}_k^{BB} \right\|_2^2 = \left\| vec\left(\mathfrak{F}^{opt}\right) - \left(I_{N_s}\otimes\mathfrak{F}^{RF}\right)\mathfrak{F}_k^{BB} \right\|_2^2$. A difficulty in (32) is that the rank constraint to transfer (32) can be formulated in standard QCQP form.

$$\min_{Ð} \left\| t\,\mathfrak{F}^{opt} - \mathfrak{I}\,Ð \right\|_2^2$$

$$s.t. \begin{cases} \|Ð\|_2^2 \leq \dfrac{\mathsf{P}_{max}}{N_t}N_{RF} \\ t^2 = 1 \end{cases} \quad (33)$$

The objective function in (33) can be expressed as follows:

$$\left\| t\,\mathfrak{F}^{opt} - \mathfrak{I}\,Ð \right\|_2^2$$

$$= \underbrace{\begin{bmatrix} Ð^H & t \end{bmatrix}}_{\mathfrak{I}}$$

$$\times \underbrace{\begin{bmatrix} \left(I_{N_s}\otimes\mathfrak{F}^{RF}\right)^H \left(I_{N_s}\otimes\mathfrak{F}^{RF}\right) & -\left(I_{N_s}\otimes\mathfrak{F}^{RF}\right)\mathfrak{f}^{opt} \\ -\left(\mathfrak{f}^{opt}\right)^H \left(I_{N_s}\otimes\mathfrak{F}^{RF}\right) & \left(\mathfrak{f}^{opt}\right)^H \mathfrak{f}^{opt} \end{bmatrix}}_{\in}$$

$$\times \underbrace{\begin{bmatrix} D \\ t \end{bmatrix}}_{\mathfrak{I}} \quad (34)$$

$$\|Ð\|_2^2$$

$$= \begin{bmatrix} Ð^H & t \end{bmatrix}$$

$$\times \underbrace{\begin{bmatrix} I\mathsf{P}_{max}N_{RF} & 0 \\ 0 & 0 \end{bmatrix}}_{\mathbb{A}_1} \begin{bmatrix} Ð \\ t \end{bmatrix} \leq \frac{\mathsf{P}_{max}}{N_t}N_{RF} \quad (35)$$

$$t^2$$

$$= \begin{bmatrix} Ð^H & t \end{bmatrix} \underbrace{\begin{bmatrix} 0\mathsf{P}_{max}N_{RF} & 0 \\ 0 & 1 \end{bmatrix}}_{\mathbb{A}_2} \begin{bmatrix} Ð \\ t \end{bmatrix} = 1 \quad (36)$$

From (34), the objective function develops in real QCQP. The special characteristic of HP $\frac{N_{RF}}{N_t}$ can find the best N_{RF} vectors or global optimal solution of the precoder design problem in (33). The digital precoding design problem in (32) is solved using the low-complexity HP for alternating minimization for the PCS structure to satisfy the power constraint and considerable gain for analog beamforming [20]. $Ð_n$ represents the values of $Ð$, $\mathfrak{I} = \begin{bmatrix} Ð \\ t \end{bmatrix}$, and $\mathfrak{k} = \mathfrak{I}^H\mathfrak{I}$. The original problem and each difference constraint can be rewritten $\left\| \mathfrak{k}_n \right\|^2$ as:

$$\min_{\mathfrak{k}\in\mathbb{U}^n} \mathfrak{I}^H \in \mathfrak{I}$$

$$s.t. \left\| \mathfrak{k}_n \right\|^2 = 1$$

$$\mathfrak{I}^H \in \mathfrak{I} \leq \frac{\mathsf{P}_{max}}{N_t}N_{RF}$$

$$rank\,\left(\mathfrak{k}\right) = 1$$

$$\mathfrak{k} \geq 0 \quad (37)$$

Subsequently, we identify:

$$\mathfrak{I} = \begin{bmatrix} Ð \\ t \end{bmatrix}, \mathfrak{k} = \mathfrak{I}^H\mathfrak{I}, \quad \in$$

$$= \begin{bmatrix} \left(I_{N_s}\otimes\mathfrak{F}^{RF}\right)^H \left(I_{N_s}\otimes\mathfrak{F}^{RF}\right) & -\left(I_{N_s}\otimes\mathfrak{F}^{RF}\right)\mathfrak{f}^{opt} \\ -\left(\mathfrak{f}^{opt}\right)^H \left(I_{N_s}\otimes\mathfrak{F}^{RF}\right) & \left(\mathfrak{f}^{opt}\right)^H \mathfrak{f}^{opt} \end{bmatrix}$$

$$\mathbb{A}_1 = \begin{bmatrix} I\mathsf{P}_{max}N_{RF} & 0 \\ 0 & 0 \end{bmatrix}, \quad \mathbb{A}_2 = \begin{bmatrix} 0\mathsf{P}_{max}N_{RF} & 0 \\ 0 & 1 \end{bmatrix}$$

$$(38)$$

We assume $\mathfrak{I}^H \in \mathfrak{I} = \mathrm{Tr}\left(\in\mathfrak{I}\,\mathfrak{I}^H\right)$. The most complex portion in (37) is the rank constraint, which is non-convex

with recognized $\mathfrak{k}$. The original problem (32) is non-convex and can be rewritten in (37) by using QCQP to obtain the relaxed version by using the dimension Hermitian matrices. We first drop (37) for the rank constraint to obtain the relaxed version by using low-complexity HP for alternating minimization as follows:

$$\min_{\mathfrak{k} \in \mathbb{w}^n} \mathrm{Tr} \ (\in \mathfrak{k})$$

$$s.t. \ \mathrm{Tr} \ (\mathbb{A}_1 \ \mathfrak{k}) = \frac{p_{max}}{N_t} N_{RF}$$

$$\mathrm{Tr} \ (\mathbb{A}_2 \ \mathfrak{k}) = 1$$

$$\mathfrak{k} \geq 0 \qquad (39)$$

where $\mathbb{w}^n$ is the set of $n = N_{RF} N_s + 1$ dimension complex Hermitian matrices. The constraint in (39) becomes convex based on the initial relaxation of the constraint condition rank $(\mathfrak{k}) = 1$ [35] if the optimization solution $\mathfrak{k}^{opt}$ does not satisfy the constraint condition according to rank $(\mathfrak{k}) = 1$ in (37). By contrast, the optimization solution $\mathfrak{k}^{opt}$ cannot be satisfied using the decomposed product between two vectors $\mathfrak{k}^{opt} = \mathfrak{T}^H \mathfrak{T}$. Therefore, the BBP $\mathfrak{F}_k^{BB}$ is solved using the approximate method in [36]–[38] by computing the uncon-straint optimal precoders of the first N_s column of $\mathbb{v}$ and $\mathbb{y}^H$. They are computed using unitary matrices grown from the channel's SVD to be decomposed as $\mathfrak{k}^{opt} = \mathbb{v} \sum \mathbb{y}^H$. The approximate solution is obtained for optimization solution $\mathfrak{k}^{opt} = \mathbb{E} \left[\mathfrak{T}^H \mathfrak{T} \right]$ for each column of $\mathbb{v}$ to be the eigenvalues of $\mathfrak{k}^{opt}$, and $\sum$ is a diagonal matrix for eigenvalues of $\mathfrak{k}^{opt}$. The corresponding solution is obtained by selecting the random vector $\mathfrak{T}$, which satisfies $\left\| \mathfrak{F}^{RF} \mathfrak{F}_k^{BB} \right\| \leq p_{max}$ by approximate solution (32). The signal phase is affected by the change in RF precoding matrix, and high EE is obtained with a relatively large N_{RF}. The power constraint is given as follows:

$$\min_{\mathfrak{F}_{RF} \in \mathbb{C}^{N_{RF} \times N_t}} \left\| \mathfrak{F}^{opt} - \mathfrak{F}^{RF} \mathfrak{F}_k^{BB} \right\|_F^2$$

$$s.t. \ \mathfrak{F}^{RF} = \mathrm{diag} \left\{ \mathfrak{f}_1, \ldots, \mathfrak{f}_{N_{RF}} \right\}$$

$$\mathfrak{F}^{RF} \mathfrak{F}_k^{BB} = \left[\mathfrak{f}_{RF, \ (\ :1)}, \ldots, \mathfrak{f}_{RF, \ (\ :N_{RF})} \right]$$

$$\times \begin{bmatrix} \mathfrak{f}_{k(1, \ :)}^{BB} \\ \cdots \\ \mathfrak{f}_{k(N_{RF}, \ :)}^{BB} \end{bmatrix}$$

$$= \sum_i^{N_{RF}} \mathfrak{f}_{RF, \ (\ :N_{RF})} \mathfrak{f}_{k(N_{RF},:)}^{BB}$$

$$\left\| \mathfrak{F}^{opt} - \mathfrak{F}^{RF} \mathfrak{F}_k^{BB} \right\|_F^2 = \frac{N_{RF} \left\| \mathfrak{F}_k^{BB} \right\|_F^2}{N_t} \leq p_{max}$$

$$\mathrm{Phase} \left(\mathfrak{F}^{opt} \right) = \mathrm{Phase} \left(\mathfrak{F}^{RF} \mathfrak{F}_k^{BB} \right) \qquad (40)$$

The value range of the element in the i th column of $\mathfrak{F}^{RF}$ to be continuous depend on applying the specified

minimization to ensure continuity (40). The optimal phase precoders Phase $\left(\mathfrak{F}^{opt} \right)$ operation is obtained with low-cost phase shifters by minimizing the Euclidean distance or a limited number of lossy connections between analog RF and BBPs of each element of the matrix.

$$\mathrm{Phase} \left(\mathfrak{F}^{RF}_{(i,j)} \right) = \mathrm{Phase} \left(\mathfrak{F}^{opt}_{(i,:)} \left(\mathfrak{F}_k^{BB} \right)^H_{(j,:)} \right),$$

$$1 \leq i \leq N_t, \ j = \left\lceil i \frac{N_{RF}}{N_t} \right\rceil \qquad (41)$$

Algorithm 3 Optimized HP-Based Alternating Minimization With Low Complexity for PCS

---

1. **Input**: $\mathfrak{F}^{opt}$
2. **Output**: $\mathfrak{F}_{op}^{BB} \ \mathfrak{F}_{op}^{RF}$
3. Create $\mathfrak{F}_i^{RF}$ with random phase, and adjust $i = 0$;
4. **Repeat**
5. Fix $\mathfrak{F}_i^{RF}$ compute $\mathfrak{F}_i^{BB}$ using (40);
6. Fix $\mathfrak{F}_i^{BB}$ and update $\mathfrak{F}_{i+1}^{RF}$ by (41);
7. **Until**
8. $i = i + 1$;
9. $\left\| \mathfrak{F}^{opt} - \mathfrak{F}_i^{RF} \mathfrak{F}_i^{BB} \right\|_F^2 < \varepsilon$ a stopping criterion is triggered;
10. $\mathfrak{F}_{op}^{BB} = \mathfrak{F}_i^{BB}, \ \mathfrak{F}_{op}^{RF} = \mathfrak{F}_i^{RF}$;

F. COMPLEXITY

The hardware has the objective of computation of high-dimensional optimal HP matrix design. The complexity for FCS based on using closed-form solutions and phase extraction for alternating minimization algorithm is equivalent to the complexity for the updating procedures of the DP parts. Furthermore, the dimension of the analog precoders is greater than that of the DPs in the HP design. This solves the complexity of the algorithms based on the analog part. The updating analog precoders need to use the zero gradient method to obtain the stationary point of optimal BBP for every iteration of the phase extraction for the alternating minimization algorithm. Every iteration is realized to provide low complexity by a phase extraction process of the matrix $\mathfrak{F}^{opt} \left(\mathfrak{F}_k^{SS} \right)^H_{(, \ i)}$ for alternating minimization by updating the analog precoders with dimension $N_t \times \mathfrak{F}_{RF}$. From (23), min-imizing the effectiveness of the limit of the upper bound is $N_s \leq N_{RF} \leq 2N_s$, and the upper bound becomes difficult when $N_{RF} = N_s$. A small performance loss is obtained when N_{RF} is increased from N_s to $2N_s - 1$ by comput-ing the gap between $\left\| \mathfrak{F}^{RF} \mathfrak{F}_k^{SS} \right\|_F^2$ and $\left\| \mathfrak{F}^{RF} \right\|_F^2$, as shown as in (23). $\left\| \mathfrak{F}^{RF} \mathfrak{F}_k^{SS} \right\|_F^2$ is substituted to $\left\| \mathfrak{F}^{RF} \mathcal{M}_1 \right\|_F^2$, where $\mathcal{M}_1$ represents the rightmost $N_{RF} - N_s$ of $\mathcal{M}$ to yield a small performance loss and reduce the computational complex-ity. When $N_{RF} \leq 2N_s$, the energy-efficient HP achieves the maximum EE.

IEEE *Access*

A. Salh *et al.*: Low Computational Complexity for Optimizing Energy Efficiency in mm-wave Hybrid Precoding System for 5G

TABLE 2. Simulation parameters.

Parameter	Value
N_t	144
N_r	36
N_{RF}	5
K	5
p_{max}	33 dBm
Power amplifier efficiency Ξ	0.38
p_C	20 W
P_{RF}	48 mW
Carrier frequency γ	28 MHz
Bandwidth ϖ	20 MHz
The number of multi-paths propagation channel $\mathcal{L}_k$	30
Noise power density α	−174 dBm/Hz
Uniform distribution	$[0, 22\pi)$

IV. SIMULATION RESULTS

This section presents simulation results to establish EE with several RF chains, the number of antennas, and some UEs. Simulation parameters are encapsulated in Table 2.
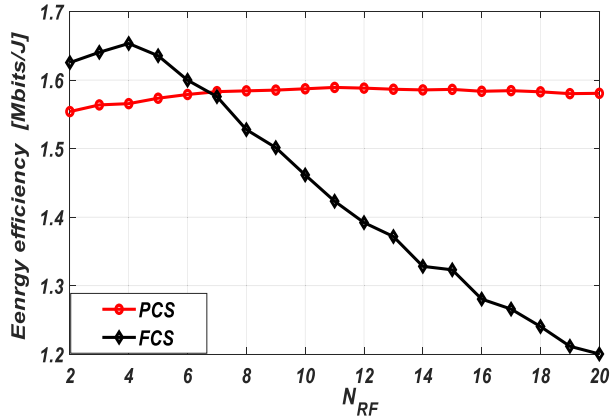
FIGURE 2. EE with respect to the number of RF chains for FCS/PCS.

Fig. 2 illustrates the different structures for FCS/PCS. The performance of EE decreases when the PC increases with a greater number of phase shifters connected with several RF chains in the FCS structure. The proposed phase extraction alternating minimization algorithm has much lower complexity as it does not allow the N_{RF} to increase. In particular, high EE provides a small N_{RF}. In PCS, the EE will be increased and produces the same values to increase the N_{RF}. Minimizing the Euclidean distance in (41) optimizes BBP and decreases the hardware complexity in the RF chains domain by employing fewer phase shifters in the analog RF precoders. Fig. 2 shows that at an intersection point for a two-HP structure, the FCS provides high EE when the N_{RF} is less than the intersection point. Meanwhile, the PCS yields high EE when the N_{RF} is implemented at transceivers. Fig. 3 shows the performance of SE with the effect of the N_{RF} evaluated by comparing different algorithms with the assumption that 6 data streams are transmitted.

The SE is achieved by introducing phase extraction as an alternative minimization when $N_{RF} \geq 2N_s$, and it will gradually approach the sufficiently close value of the optimal
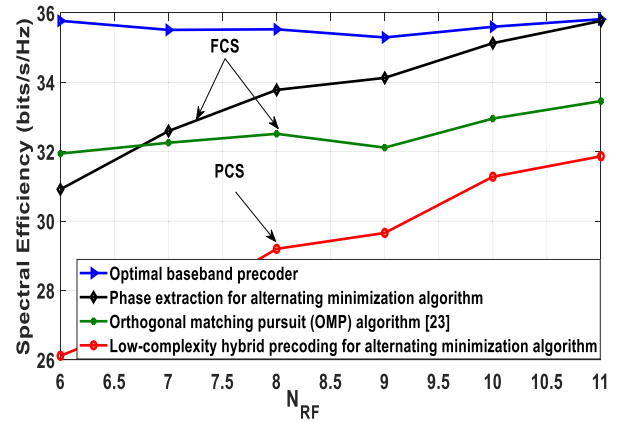

FIGURE 3. Comparison of different precoding algorithms in terms of SE.

BBP. As depicted in Fig. 3, the SE improves in the PCS for the region $N_{RF} \in [6, 11]$. When N_{RF} increases, the PC remains unchanged because the low-complexity algorithm reduces an upper bound.
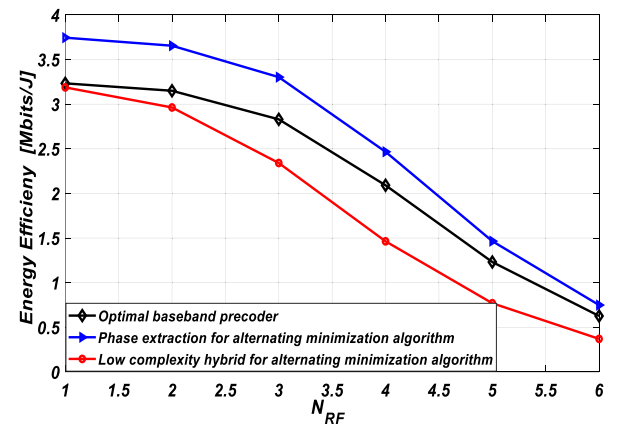

FIGURE 4. EE versus the number of RF.

In the FCS, the SE enhances upon slightly increasing an N_{RF} by applying the proposed phase extraction alternating minimization algorithm with the optimal BBPs when the N_{RF} is larger than $2N_s$. When the N_{RF} is smaller, the OMP algorithm provides high SE. When the N_{RF} is increased, the phase extraction and alternative minimization provide higher SE than OMP. Therefore, the phase extraction of the FCS approaches to the optimal BBPs when the N_{RF} is equivalent to N_s. Fig. 4 shows that EE starts to decrease when the N_{RF} for FCS/PCS is increased. The EE with FCS/PCS algorithms can always maintain the best performance with a large N_{RF}. The phase extraction of an alternative minimization in FCS provides the best EE performance when the N_{RF} is between 4 and 6. It sufficiently approaches the close value of the optimal BBPs when the N_{RF} is increased. However, the large gains over analog beamforming are obtained to avoid the high energy consumption in low-complexity HP for alternating minimization algorithm. The proposed optimal BBP algorithms provide higher EE than the two other proposed algorithms when the N_{RF} is between 1 and 6.
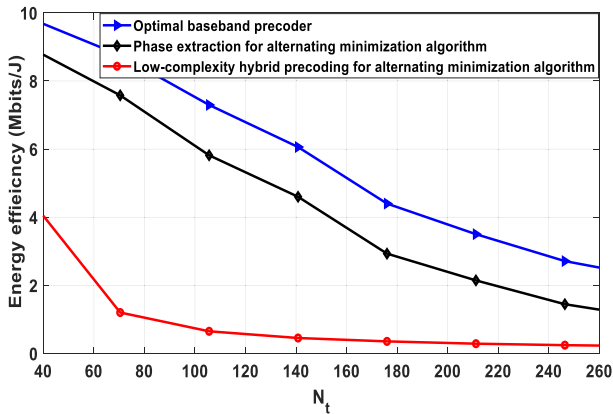
A. Salh *et al.*: Low Computational Complexity for Optimizing Energy Efficiency in mm-wave Hybrid Precoding System for 5G

IEEE*Access*

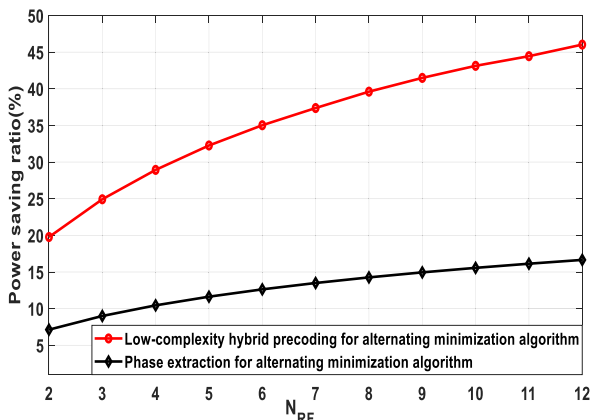**FIGURE 5.** EE comparison against the number of antennas N_t.

FIGURE 6. Power-saving ratio with respect to the number of RF chains.

Fig. 5 presents the performance of EE concerning the number of transmission antennas (N_t). The EE for different precoding algorithms decreases with the increase in the N_t according to the computation power in an mMIMO system. When N_t is fixed, the optimal BBP provides larger EE than FCS and PCS. The FCS provides a higher EE in terms of hardware complexity and communication power than PCS. Fig. 6 shows the related power-saving ratio concerning the N_{RF}. The PC of the phase extraction FCS increases when the N_{RF} is large. When the N_{RF} is 12, the power-saving ratio is 48.3% in low-complexity HP for alternating minimization algorithm. The power-saving ratio is 17.12% for the FCS of phase extraction as an alternative minimization at the same N_{RF} of 12. The high power-saving ratio is more difficult to obtain when the system employs power gain for interference control. The PCS can provide good performance with higher EE. The low-complexity HP for alternating minimization algorithm assigns power to different RF chains and breaches the per RF power limit. As shown in Fig. 7, the EE with different precoding algorithms increases when the number of UEs is small. Thereafter, the EE starts to decrease with the increase in UEs. The optimal BBPs provide higher EE than the two proposed algorithms when the N_{RF} is between 1 and 12. When the number of UEs is more than 6, PCS's low-complexity HP can achieve fairly satisfactory performance and provides a larger EE than phase extraction in

FCS. Moreover, when the number of UEs is small, the phase extraction in FCS gradually approaches the sufficiently close value of the optimal BBPs.
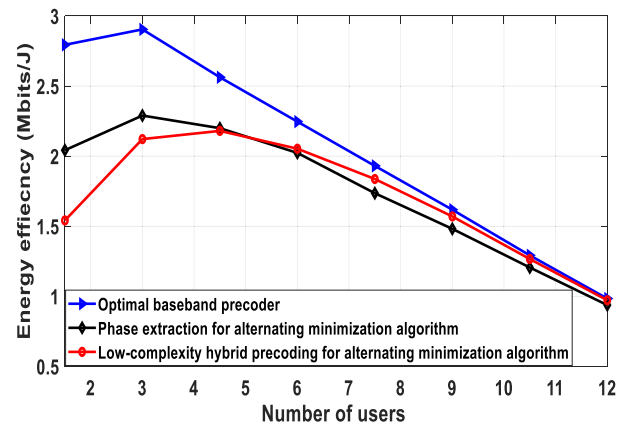

FIGURE 7. Performance of EE with respect to the number of users.
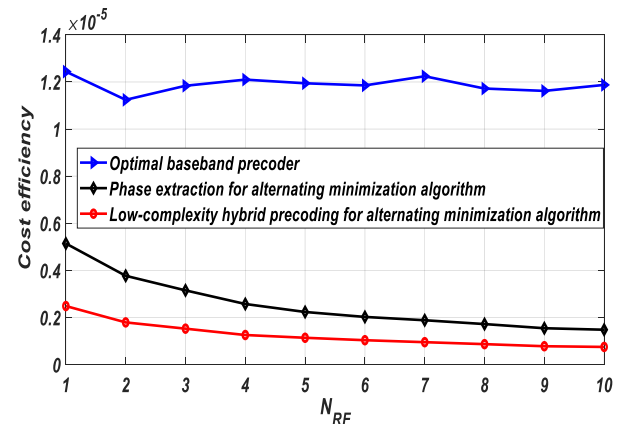

FIGURE 8. Cost efficiency concerning the number of RF chains.

Therefore, the FCS/PCS architectures with dynamic sub-array and low-resolution phase shifters effectively reduce the number of phase shifters and improve the EE. Fig. 8 shows that the cost efficiency decreases when the N_t increases in MU - mMIMO systems. The cost efficiency of optimal BBPs also improves when the N_t is increased. Meanwhile, the phase extraction in FCS and low-complexity HP for alternating minimization algorithm decreases with the increase in the N_t. The maximum cost efficiency improved with FCS structures during each iteration is achieved to deliver the low complexity by a phase extraction process of the matrix $\mathbb{F}^{opt}\left(\mathbb{F}_k^{SS}\right)^H_{(,:\,i)}$.

V. CONCLUSION

In this paper, we propose alternating minimization for a HP- mm-wave mMIMO system. We jointly optimize the communication power of RF systems to minimize the cost and complexity of MU- mMIMO systems. The performance of *EE* decreases when the N_{RF} N_{RF} increases. The EE with FCS/PCS algorithms can always maintain the best performance of EE = 3.7 Mbits/J and decreases the EE

IEEE *Access*

A. Salh *et al.*: Low Computational Complexity for Optimizing Energy Efficiency in mm-wave Hybrid Precoding System for 5G

to 2.9 Mbits/J with increases the N_{RF}. Moreover, when the N_{RF} is greater than the N_s, the HPs with the FCS can move toward the optimal BBPs. The PCS improves EE and SE with a relatively large N_{RF}. The proposed algorithms for FCS/PCS are developed to optimize the performance of the MU - mMIMO communication system. The simulation results show that the proposed low-complexity HP for alternating minimization algorithm in FCS and PCS achieves 48.3% and 17.12%, respectively. The PCS structure becomes better than the phase extraction for alternating minimization algorithm in FCS in terms of cost efficiency and maximum power-saving ratio. In the future, due to high-computational complexity and failure to fully exploit mm-wave spatial information. So we plan to construct selected training data sequences based on the DNN for optimizing the precoding process of the mm-wave mMIMO to explore the trade-off between energy and cost efficiency, depending on the deep learning approach that facilitates dynamic power allocation improve the performance channel training and provide less computation time.

REFERENCES

[1] A. Ghosh, R. Ratasuk, B. Mondal, N. Mangalvedhe, and T. Thomas, "LTE-advanced: Next-generation wireless broadband technology," *IEEE Wireless Commun.*, vol. 17, no. 3, pp. 10–22, Jun. 2010.

[2] D. Lopez-Perez, I. Guvenc, G. de la Roche, M. Kountouris, T. Q. S. Quek, and J. Zhang, "Enhanced intercell interference coordination challenges in heterogeneous networks," *IEEE Wireless Commun.*, vol. 18, no. 3, pp. 22–30, Jun. 2011.

[3] M. R. Akdeniz, Y. Liu, M. K. Samimi, S. Sun, S. Rangan, T. S. Rappaport, and E. Erkip, "Millimeter wave channel modeling and cellular capacity evaluation," *IEEE J. Sel. Areas Commun.*, vol. 32, no. 6, pp. 1164–1179, Apr. 2013.

[4] Z. Pi and F. Khan, "An introduction to millimeter-wave mobile broadband systems," *IEEE Commun. Mag.*, vol. 49, no. 6, pp. 101–107, Jun. 2011.

[5] Y.-Y. Lee, C.-H. Wang, and Y.-H. Huang, "A hybrid RF/baseband precoding processor based on parallel-index-selection matrix-inversion-bypass simultaneous orthogonal matching pursuit for millimeter wave MIMO systems," *IEEE Trans. Signal Process.*, vol. 63, no. 2, pp. 305–317, Jan. 2015.

[6] C. Rusu, R. Mendez-Rial, N. Gonzalez-Prelcicy, and R. W. Heath, Jr., "Low complexity hybrid sparse precoding and combining in millimeter wave MIMO systems," in *Proc. IEEE Int. Conf. Commun. (ICC)*, London, U.K., Jun. 2015, pp. 1340–1345.

[7] L. N. Ribeiro, S. Schwarz, M. Rupp, and A. L. de Almeida, "Energy efficiency of mmWave massive MIMO precoding with low-resolution DACs," *IEEE J. Sel. Topics Signal Process.*, vol. 12, no. 2, pp. 298–313, May 2018.

[8] C. Rusu, R. Mèndez-Rial, N. González-Prelcic, and R. W. Heath, Jr., "Low complexity hybrid precoding strategies for millimeter wave communication systems," *IEEE Trans. Wireless Commun.*, vol. 15, no. 12, pp. 8380–8393, Dec. 2016.

[9] C.-E. Chen, "An iterative hybrid transceiver design algorithm for millimeter wave MIMO systems," *IEEE Wireless Commun. Lett.*, vol. 4, no. 3, pp. 285–288, Jun. 2015.

[10] W. Hao, G. Sun, F. Zhou, D. Mi, J. Shi, P. Xiao, and V. C. M. Leung, "Energy-efficient hybrid precoding design for integrated multicast-unicast millimeter wave communications with SWIPT," *IEEE Trans. Veh. Technol.*, vol. 68, no. 11, pp. 10956–10968, Nov. 2019.

[11] W. Ni and X. Dong, "Hybrid block diagonalization for massive multiuser MIMO systems," *IEEE Trans. Commun.*, vol. 64, no. 1, pp. 201–211, Jan. 2016.

[12] R. Zi, X. Ge, J. Thompson, C.-X. Wang, H. Wang, and T. Han, "Energy efficiency optimization of 5G radio frequency chain systems," *IEEE J. Sel. Areas Commun.*, vol. 34, no. 4, pp. 758–771, Apr. 2016.

[13] X. Xue, Y. Wang, L. Yang, J. Shi, and Z. Li, "Energy-efficient hybrid precoding for massive MIMO mmWave systems with a fully-adaptive-connected structure," *IEEE Trans. Commun.*, vol. 68, no. 6, pp. 3521–3535, Jun. 2020.

[14] D. Zhang, Y. Wang, X. Li, and W. Xiang, "Hybridly connected structure for hybrid beamforming in mmWave massive MIMO systems," *IEEE Trans. Commun.*, vol. 66, no. 2, pp. 662–674, Feb. 2018.

[15] X. Yu, J.-C. Shen, J. Zhang, and K. B. Letaief, "Alternating minimization algorithms for hybrid precoding in millimeter wave MIMO systems," *IEEE J. Sel. Topics Signal Process.*, vol. 10, no. 3, pp. 485–500, May 2016.

[16] J. Lee, G. T. Gil, and Y. H. Lee, "Channel estimation via orthogonal matching pursuit for hybrid MIMO systems in millimeter wave communications," *IEEE Trans. Commun.*, vol. 64, no. 6, pp. 86–2370, Apr. 2016.

[17] H. Li, M. Li, and Q. Liu, "Hybrid beamforming with dynamic subarrays and low-resolution PSs for mmWave MU-MISO systems," *IEEE Trans. Commun.*, vol. 68, no. 1, pp. 602–614, Jan. 2020.

[18] N. Li, Z. Wei, H. Yang, X. Zhang, and D. Yang, "Hybrid precoding for mmWave massive MIMO systems with partially connected structure," *IEEE Access*, vol. 5, pp. 15142–15151, 2017.

[19] S. He, C. Qi, Y. Wu, and Y. Huang, "Energy-efficient transceiver design for hybrid sub-array architecture MIMO systems," *IEEE Access*, vol. 4, pp. 9895–9905, 2017.

[20] C. Lin and G. Y. Li, "Energy-efficient design of indoor mmWave and sub-THz systems with antenna arrays," *IEEE Trans. Wireless Commun.*, vol. 15, no. 7, pp. 4660–4672, Jul. 2016.

[21] A. Salh, L. Audah, N. S. M. Shah, and S. A. Hamzah, "Energy-efficient power allocation with hybrid beamforming for millimetre-wave 5G massive MIMO system," *Wireless Pers. Commun.*, vol. 115, no. 1, pp. 43–59, Nov. 2020.

[22] T. E. Bogale and L. B. Le, "Beamforming for multiuser massive MIMO systems: Digital versus hybrid analog-digital," in *Proc. IEEE Global Commun. Conf.*, Austin, TX, USA, Dec. 2014, pp. 4066–4071.

[23] H. Q. Ngo, E. G. Larsson, and T. L. Marzetta, "Energy and spectral efficiency of very large multiuser MIMO systems," *IEEE Trans. Commun.*, vol. 61, no. 4, pp. 1436–1449, Apr. 2013.

[24] D. Ha, K. Lee, and J. Kang, "Energy efficiency analysis with circuit power consumption in massive MIMO systems," in *Proc. IEEE 24th Annu. Int. Symp. Pers., Indoor, Mobile Radio Commun. (PIMRC)*, London, U.K., Sep. 2013, pp. 938–942.

[25] T. L. Marzetta, "Noncooperative cellular wireless with unlimited numbers of base station antennas," *IEEE Trans. Wireless Commun.*, vol. 9, no. 11, pp. 3590–3600, Nov. 2010.

[26] A. Alkhateeb, O. El Ayach, G. Leus, and R. W. Heath, Jr., "Channel estimation and hybrid precoding for millimeter wave cellular systems," *IEEE J. Sel. Topics Signal Process.*, vol. 8, no. 5, pp. 831–846, Oct. 2014.

[27] W. U. Bajwa, J. Haupt, A. M. Sayeed, and R. Nowak, "Compressed channel sensing: A new approach to estimating sparse multipath channels," *Proc. IEEE*, vol. 98, no. 6, pp. 1058–1076, Jun. 2010.

[28] X. Gao, L. Dai, S. Han, I. Chih-Lin, and R. W. Heath, Jr., "Energy-efficient hybrid analog and digital precoding for mmWave MIMO systems with large antenna arrays," *IEEE J. Sel. Areas Commun.*, vol. 34, no. 4, pp. 998–1009, Apr. 2016.

[29] X. Ge, Y. Sun, H. Gharavi, and J. Thompson, "Joint optimization of computation and communication power in multi-user massive MIMO systems," *IEEE Trans. Wireless Commun.*, vol. 17, no. 6, pp. 4051–4063, Jun. 2018.

[30] J. Jing, C. Xiaoxue, and X. Yongbin, "Energy-efficiency based downlink multi-user hybrid beamforming for millimeter wave massive MIMO system," *J. China Universities Posts Telecommun.*, vol. 23, no. 4, pp. 53–62, Aug. 2016.

[31] C. Jiang and L. J. Cimini, "Downlink energy-efficient multiuser beamforming with individual SINR constraints," in *Proc. Mil. Commun. Conf. (MILCOM)*, Baltimore, MD, USA, Nov. 2011, pp. 495–500.

[32] C. Jiang and L. J. Cimini, "Energy-efficient transmission for MIMO interference channels," *IEEE Trans. Wireless Commun.*, vol. 12, no. 6, pp. 2988–2999, Jun. 2013.

[33] S. W. Peters and R. W. Heath, "Interference alignment via alternating minimization," in *Proc. IEEE Int. Conf. Acoust., Speech Signal Process.*, Taipei, Taiwan, Apr. 2009, pp. 2445–2448.

[34] Y. Pu, M. N. Zeilinger, and C. N. Jones, "Complexity certification of the fast alternating minimization algorithm for linear MPC," *IEEE Trans. Autom. Control*, vol. 62, no. 2, pp. 888–893, Feb. 2017.

[35] Z.-Q. Luo, W.-K. Ma, A. M.-C. So, Y. Ye, and S. Zhang, "Semidefinite relaxation of quadratic optimization problems," *IEEE Signal Process. Mag.*, vol. 27, no. 3, pp. 20–34, May 2010.

A. Salh *et al.*: Low Computational Complexity for Optimizing Energy Efficiency in mm-wave Hybrid Precoding System for 5G

IEEE *Access*

[36] H. Hoilund-Kaupang and S.-E. Masoy, "Transmit beamforming for optimal second-harmonic generation," *IEEE Trans. Ultrason., Ferroelectr., Freq. Control*, vol. 58, no. 8, pp. 1559–1569, Aug. 2011.

[37] J. Liu, H. Deng, S. Wang, G. Liu, K. Yang, and Z. Zhu, "Initial value acceleration-based alternating minimization algorithm for dynamic sub-connected hybrid precoding in millimeter wave MIMO systems," *Symmetry*, vol. 13, pp. 1–14, Feb. 2021.

[38] A. N. Mohammed and I. Kostanic, "Low computational complexity and minimizing training overhead for hybrid precoding in millimeter wave systems," in *Proc. Texas Symp. Wireless Microw. Circuits Syst. (WMCS)*, Waco, TX, USA, Apr. 2018, pp. 1–5.

MOHAMMED A. ALHARTOMI (Member, IEEE) received the Ph.D. degree in electronic and electrical engineering from the University of Leeds, U.K., in 2016. He is currently an Assistant Professor with the Department of Electrical Engineering, University of Tabuk. His research interests include wireless and mobile communications, signal processing, optical wireless systems design, and visible light communications.

ADEB SALH received the bachelor's degree in electrical and electronic engineering from IBB University, Ibb, Yemen, in 2007, and the master's and Ph.D. degrees in electrical and electronic engineering from Universiti Tun Hussein Onn Malaysia, Malaysia, in 2015 and 2020, respectively. He is currently a Postdoctoral Researcher at the Faculty of Electrical and Electronic Engineering, Universiti Tun Hussein Onn Malaysia.

LUKMAN AUDAH received the Bachelor of Engineering degree in telecommunications from Universiti Teknologi Malaysia, in 2005, and the M.Sc. degree in communication networks and software and the Ph.D. degree in electronic engineering from the University of Surrey, U.K. He is currently a Senior Lecturer with the Communication Engineering Department, Universiti Tun Hussein Onn Malaysia. His research interests include wireless and mobile communications, internet traffic engineering, network system management, data security, and satellite communications.

SAEED HAMOOD ALSAMHI received the B.Eng. degree from the Communication Division, Department of Electronic Engineering, IBB University, Yemen, in 2009, and the M.Tech. degree in communication systems and the Ph.D. degree from the Department of Electronics Engineering, Indian Institute of Technology Banaras Hindu University (BHU), Varanasi (IIT BHU), India, in 2012 and 2015, respectively. In 2009, he worked as an Assistant Lecturer at the engineering's faculty at IBB University. He held a postdoctoral position with the School of Aerospace Engineering, Tsinghua University, Beijing, China, in optimal and smart wireless network research and its applications to enhance robotics technologies. Since 2019, he has been an Assistant Professor at the Shenzhen Institute of Advanced Technology (SIAT), Chinese Academy of Sciences (CAS), Shenzhen, China. He has published more than 30 articles in high reputation journals in IEEE, Elsevier, Springer, Wiley, and MDPI publishers. His research interests include green communication, green Internet of Things, QoE, QoS, multi-robot collaboration, blockchain technology, and space technologies (high altitude platform, drone, and tethered balloon technologies). He is currently a MSCA SMART 4.0 Fellow at the Technological University of the Shannon: Midlands Midwest, Athlone, Westmeath, Ireland.

QAZWAN ABDULLAH (Graduate Student Member, IEEE) was born in Taiz, Yemen. He received the bachelor's degree in electrical and electronic engineering and the master's degree in science (electrical and electronic engineering) from Universiti Tun Hussein Onn Malaysia (UTHM), in 2013 and 2015, respectively. Currently, he is a Research Assistant with research interests that include control theory, adaptive fuzzy logic controller, mobile communication (5G/6G), fuzzy logic control and its applications, motor drive, electric vehicle, and antenna filter design. He has more than 40 scientific publications.

FARIS A. ALMALKI is an Assistant Professor in wireless communication satellites and drones systems at the Department of Computer Engineering, College of Computers and Information Technology, Taif University, Saudi Arabia. He received a postgraduate scholarship in the U.K. for a period of seven years from the Taif University Vice Presidency for Graduate Studies and Scientific Research. He is interested in volunteerism, entrepreneurship, digital media, professional development, and 21st century skills.

ÖMER AYDOĞDU was born in Konya, Turkey, in 1973. He received the B.S., M.S., and Ph.D. degrees in electrical and electronics engineering from Selçuk University, Konya, in 1995, 1999, and 2006, respectively. From 1996 to 2007, he was a Research Assistant with the Department of Electrical and Electronics Engineering, Selçuk University, where he worked as an Assistant Professor and an Associate Professor with the Department of Electrical and Electronics Engineering, from 2007 to 2018. From 2018 to 2020, he worked as an Associate Professor with the Department of Electrical and Electronics Engineering, Konya Technical University, Konya, where he has been a Professor, since 2020. He is the author of a book chapter and more than 70 scientific publications. His research interests include control theory, adaptive control systems, fractional order control, fuzzy logic control and applications, and brushless dc motors and drives.

NOR SHAHIDA M. SHAH received the B.Eng. degree in electrical and electronic from the Tokyo Institute of Technology, Japan, in 2000, the M.Sc. degree in optical communication from the University of Malaya, Malaysia, in 2003, and the Ph.D. degree in electrical, electronics, and system engineering from Osaka University, Japan, in 2012. She is currently a Senior Lecturer at Universiti Tun Hussein Onn Malaysia. Her research interests include optical and wireless communication.

• • •